SUPPLEMENTARY TABLES, FIGURES AND FIGURE LEGENDS

Table S1. Status and frequencies of chromosome 17p copy number variation (CNV) across different NB clinical subtypes.

WGS profiles (135)												
	HR-AMP		**HR-NA**		**INTR**		**LOWR**			**TOTAL**	
LOSS	**9**	31.0%	**14**	18.2%	**0**	0.0%	**1**	6.7%		**24**	17.8%
NEUTRAL	**17**	58.6%	**47**	61.0%	**8**	57.1%	**1**	6.7%		**73**	54.1%
GAIN	**3**	10.3%	**16**	20.8%	**6**	42.9%	**13**	86.7%		**38**	28.1%
Total	**29**	100.0%	**77**	100.0%	**14**	100.0%	**15**	100.0%		**135**	100.0%

SNP arrays (914)												
	HR-AMP		**HR-NA**		**INTR**		**LOWR**		**Unknown**		**TOTAL**	
LOSS	**29**	12.1%	**49**	10.7%	**1**	1.4%	**4**	2.8%	**1**	33.3%	**84**	9.2%
NEUTRAL	**176**	73.6%	**288**	63.0%	**25**	35.7%	**29**	20.0%	**1**	33.3%	**519**	56.8%
GAIN	**34**	14.2%	**120**	26.3%	**44**	62.9%	**112**	77.2%	**1**	33.3%	**311**	34.0%
Total	**239**	100.0%	**457**	100.0%	**70**	100.0%	**145**	100.0%	**3**	100.0%	**914**	100.0%

HR-AMP, high-risk NB with *MYCN* amplification; HR-NA, high-risk NB without *MYCN* amplification; INTR, intermediate-risk NB; and LOWR, low-risk NB.

Table S2. Survival status of mice injected with control or *GAS7*-knockdown BE(2)-M17 cells during 11 weeks of observation period.

	Xenograft with control cells (n=12)		Xenograft with *GAS7*-knockdown cells (n=12)	
	Number s of live mice	Numbers of dead mice	Numbers of live mice	Numbers of dead mice
Week 1-6	12	0	12	0
Week 7	12	0	10	2
Week 9	12	0	9	1
Week 10	11	1	6	3
Week 11 (end of experiment)	0	11	0	6

Table S3. Primers for PCR analyses.

Human Genes	Forward Primers	Reverse Primers
ACTIN	AGAGCTACGAGCTGCCTGAC	AGCACTGTGTTGGCGTACAG
CADM3	GAACCAACCCGCATACAGGA	GCGTTGAGAGGTGGATCTGT
CDH11	GCCCCAAGTTACATCCACGA	TTGGCTTCCTGATGCCGATT
CDH6	TCAAGCCAAGGATATGGGCG	CGTCGCTGGCTTTGATTCTG
GAS7	CTCTCAGAACTCCTTGGCTTCAC	GTTCTCACGGAAGTTCATCAGGG
MYCN	ATGCACCCCCACAGAAGAAG	GAAGCGTCTAGCAAGTCCGA
GAS7 site I	CGGGGAAATAGACCCAAAGGT	TCTGGTGATACCCAATGTCAGTC
GAS7 site II	TCCCGCCTAAAACACAGTGG	CCTTCCAAATCCGCTCCAGT
GAS7 site III	TGTGCCATGGTAAAGAGGCA	TAGGGGAGCCAAGACTTCCT
SDHA	TGGGAACAAGAGGGCATCTG	CCACCACTGCATCAAATTCATG
HPRT1	TGACACTGGCAAAACAATGCA	GGTCCTTTTCACCAGCAAGCT
Mouse Gapdh	AGAACCTGCAGCCATCAGCTA	ACCTCCACTTTATAACCGTGCT
Zebrafish Genes	Forward Primers	Reverse Primers
elfa	CTTCTCAGGCTGACTGTGC	CCGCTAGCATTACCCTCC
cadm3	GGTACCGTGACCATGTGGAG	GACAGCGTGAGTTCGCTAGT
cdh11	TTCGGACAGCTCTTCCCAAC	GCCGTCTCCCTCTAAGATGC
cdh6	CCGGATCAGTGTCGAGGATG	CCGTTCCCAGCGTAGATACC
gas7 (PCR1)	CACACCCGGTCCTCCAATAC	GCCAGTTCAAGCCGTAGTCT
gas7 (PCR2)	ACCCCAAGAAAGAAGCAA	CCCAGACAAAAAGCCTAAAA

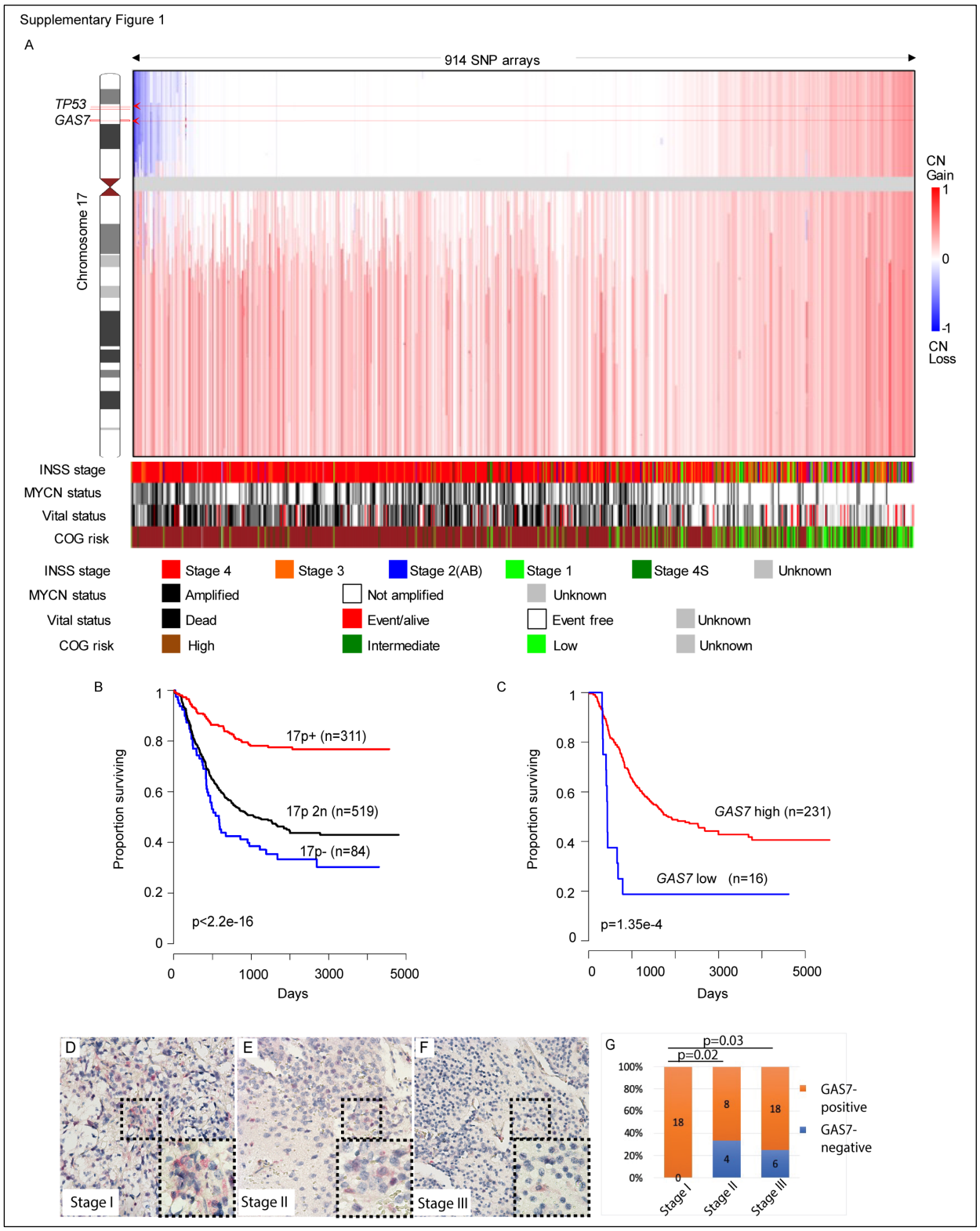
Supplementary Figure 1
A
914 SNP arrays
TP53
GAS7
Chromosome 17
CN Gain
1
0
-1
CN Loss
INSS stage
MYCN status
Vital status
COG risk
INSS stage Stage 4 Stage 3 Stage 2(AB) Stage 1 Stage 4S Unknown
MYCN status Amplified Not amplified Unknown
Vital status Dead Event/alive Event free Unknown
COG risk High Intermediate Low Unknown
B
Proportion surviving
17p+ (n=311)
17p 2n (n=519)
17p- (n=84)
p<2.2e-16
Days
C
Proportion surviving
GAS7 high (n=231)
GAS7 low (n=16)
p=1.35e-4
Days
D
Stage I
E
Stage II
F
Stage III
G
p=0.03
p=0.02
GAS7-positive
GAS7-negative
Stage I
Stage II
Stage III

Supplementary Figure 1: Bioinformatics analysis of multiple NB datasets showing association of 17p loss or low levels of *GAS7* expression with poor disease outcome of NB patients. (A) Integrative genome viewer visualization of chromosome 17 copy number across 914 primary human NBs of SNP array cohort in TARGET. Samples are ordered according to overall 17p copy number. **(B)** Kaplan-Meier survival curves demonstrating the relationship between the survival of NB patients in SNP array cohort with different 17p copy numbers, including 17p deletion (17p-), 17p neutral copy (17p 2n) and 17p gain (17p+). Differences between the curves are significant by log-rank test at p<2.2e-16. **(C)** Kaplan-Meier survival curves for NB patients stratified by *GAS7* gene expression (Human exon arrays cohort in TARGET). The difference between the curves for *GAS7*-low versus *GAS7*-high expression is significant by the log-rank test at p= 1.35e-4. **(D-F)** Immunohistochemical analysis of GAS7 expression on tissue arrays with different stages of human NBs (Cat# NB642 from US Biomax). Enlarged boxed regions are shown on the lower right corner within the same figure. **(G)** Percentage of tumors with GAS7-positive staining in each stratified stage of NB. The differences between groups are significant by Fisher's exact test at p=0.02 or p=0.03, respectively.

Supplementary Figure 2

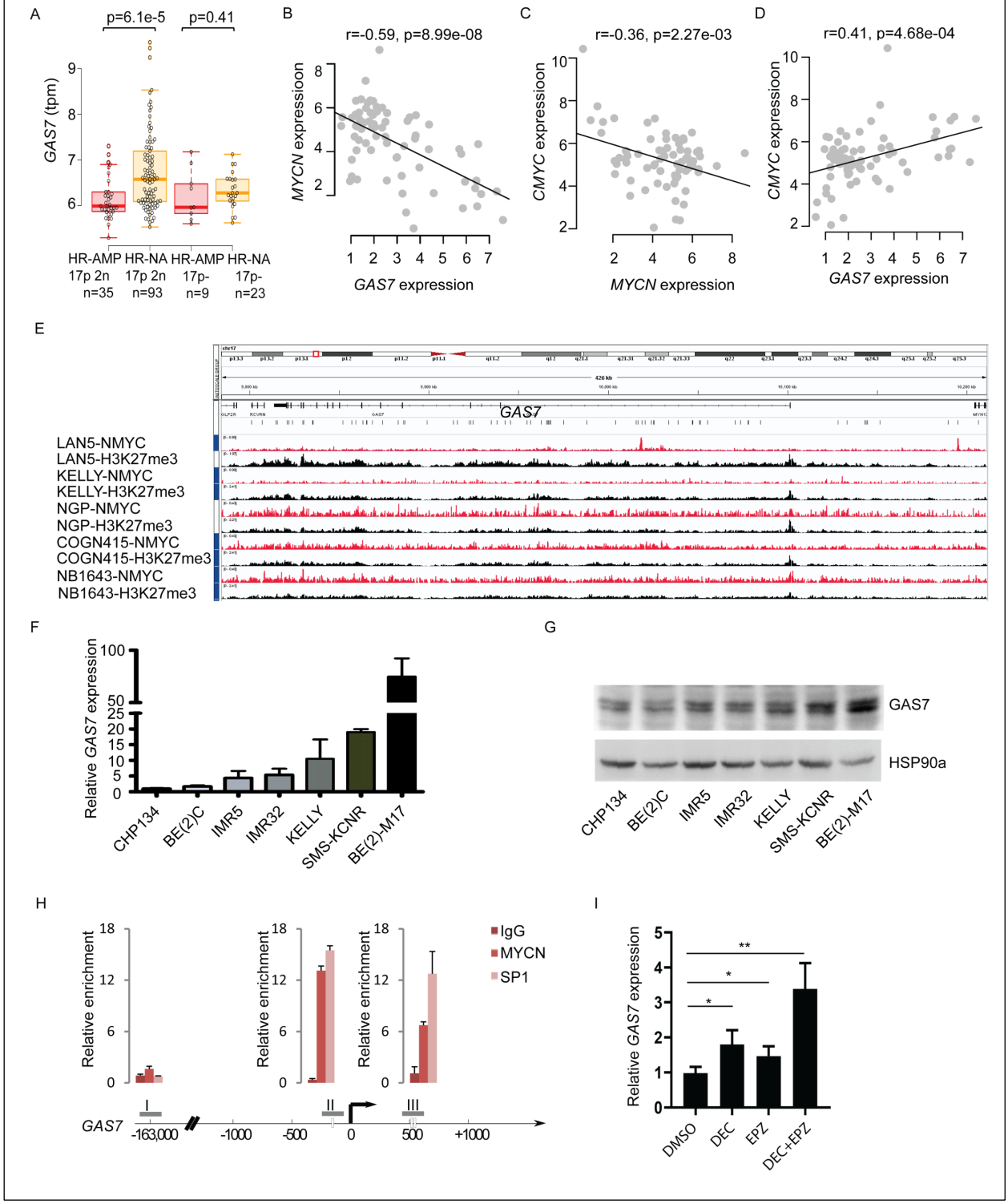

Supplementary Figure 2: *GAS7* expression is suppressed by MYCN in both human NBs and NB cell lines derived from NB patients. (A) Box plots comparing expression levels of *GAS7* in high-risk tumors with *MYCN* amplification (HR-AMP) versus those without *MYCN* amplification (HR-NA) in the context of copy number-neutral 17p (17p 2n) or loss (17p-). p=6.1e-5, by Wilcoxon rank-sum test (Human exon arrays cohort in TARGET). **(B-D)** Relationship between *GAS7*, *MYCN* and *CMYC* in *MYCN* non-amplified high-risk neuroblastoma with intact 17p (17p 2n) by Pearson's correlation analyses. Data are from Gene Expression Omnibus: GSE62564. **(E)** Snapshot of MYCN and H3K27me3 ChIP-sequencing plots showing no significant binding of MYCN to the upstream of *GAS7* in *MYCN*-amplified NB cell lines, including LAN5, Kelly, NGP, COGN415 and NB-1643. Data is from GEO database, accession number GSE94782. **(F)** Relative expression of *GAS7* versus *ACTIN* in a panel of human NB cell lines by qRT-PCR analysis. **(G)** Expression of GAS7 protein in a panel of human NB cell lines by immunoblot analysis. **(H)** Dual cross-linking ChIP-PCR with CHP-134 human NB cell line showing co-occupancy of SP1 and MYCN at two regions (II and III) of the *GAS7* promoter (region I serves as a negative control). Arrow marks the transcription start site. Experiments were performed in duplicate; and error bars represent SEM. **(I)** Relative expression of *GAS7* versus *SDHA* in BE(2)C human NB cell line in the presence or absence of decitabine/5-aza-2'-deoxycytidine (DEC, a DNA methyltransferase inhibitor), or EPZ-6438/tazemetostat (EPZ, a selective EZH2 inhibitor) alone or in combination by semiquantitative RT-PCR analysis. The data are presented as means ± SD of triplicate experiments; *$p < 0.05$ and **$p < 0.01$ by two-tailed *t* test.

Supplementary Figure 3

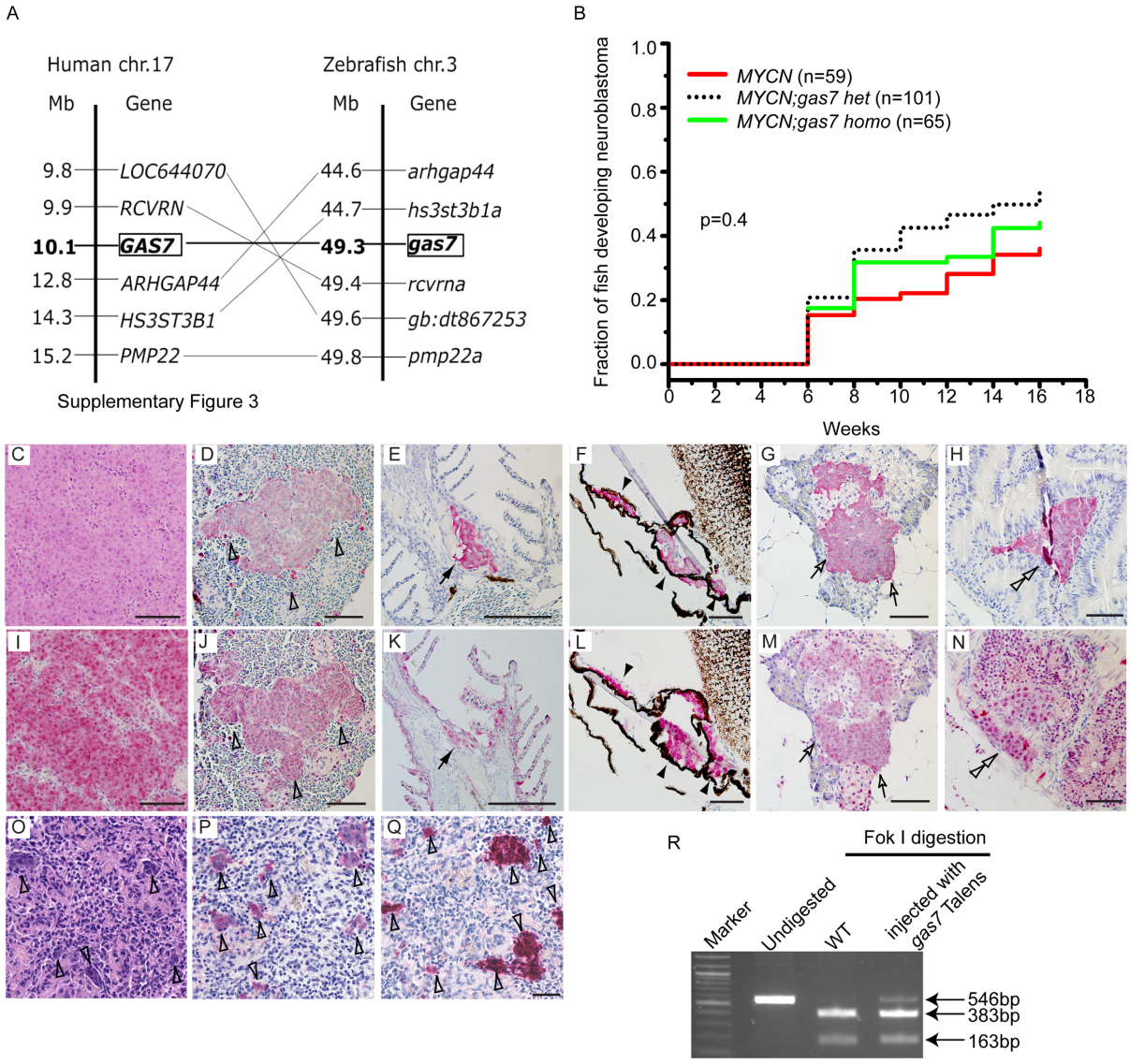

Supplementary Figure 3: Knockout of *gas7* promotes NB metastasis in transgenic fish overexpressing *MYCN*. (A) Synteny analysis of zebrafish *gas7* gene and its human homolog. Schematic representation shows genes of syntenic group within 9.8-15.2 Mb on human chromosome 17 and 44.6-49.8 Mb on zebrafish chromosome 3. Lines indicate the syntenic genes in zebrafish and human. **(B)** Kaplan-Meier analysis of the cumulative frequency of NB induction over 16 weeks in *MYCN*-only transgenic fish (*MYCN*), *MYCN* transgenic fish with heterozygous knockout of *gas7* (*MYCN;gas7mut het*), and *MYCN* transgenic fish with homozygous knockout of *gas7* (*MYCN;gas7mut homo*). Differences in the time of tumor onset were not significant by log-rank test (p=0.4, for all comparisons). **(C-N)** Magnified views of immunohistochemical analyses of sagittal sections of a 5-months old *MYCN;gas7mut homo* compound fish, using antibodies against tyrosine hydroxylase (TH) (C-H) or HuC (I-N). Tumor cells were detected in the primary site, interrenal gland (IRG) (C and I), and metastatic sites, including the spleen (D and J, open arrowheads); the gill (E and K, black arrows); the sclera of the eye (F and L, black arrowheads); the pancreas (G and M, open arrows); and the gut (H and N, double open arrowheads). Scale bars, 50 μm. **(O-Q)** Pathologic and immunohistochemical analyses of the sagittal sections of the spleen of a 6-months old *MYCN* transgenic fish raised from the embryos injected with *gas7* TALENs. O, H&E staining; P and Q, IHC staining with antibodies against GFP (P) or Tyrosine hydroxylase (TH, Q). Open arrowheads point to the disseminated tumor cells. Scale bars, 50 μm. **(R)** Gel electrophoresis demonstrating the disruption of *gas7* in the *MYCN* fish subjected for the pathological and immunohistochemical analyses.

Supplementary Figure 4

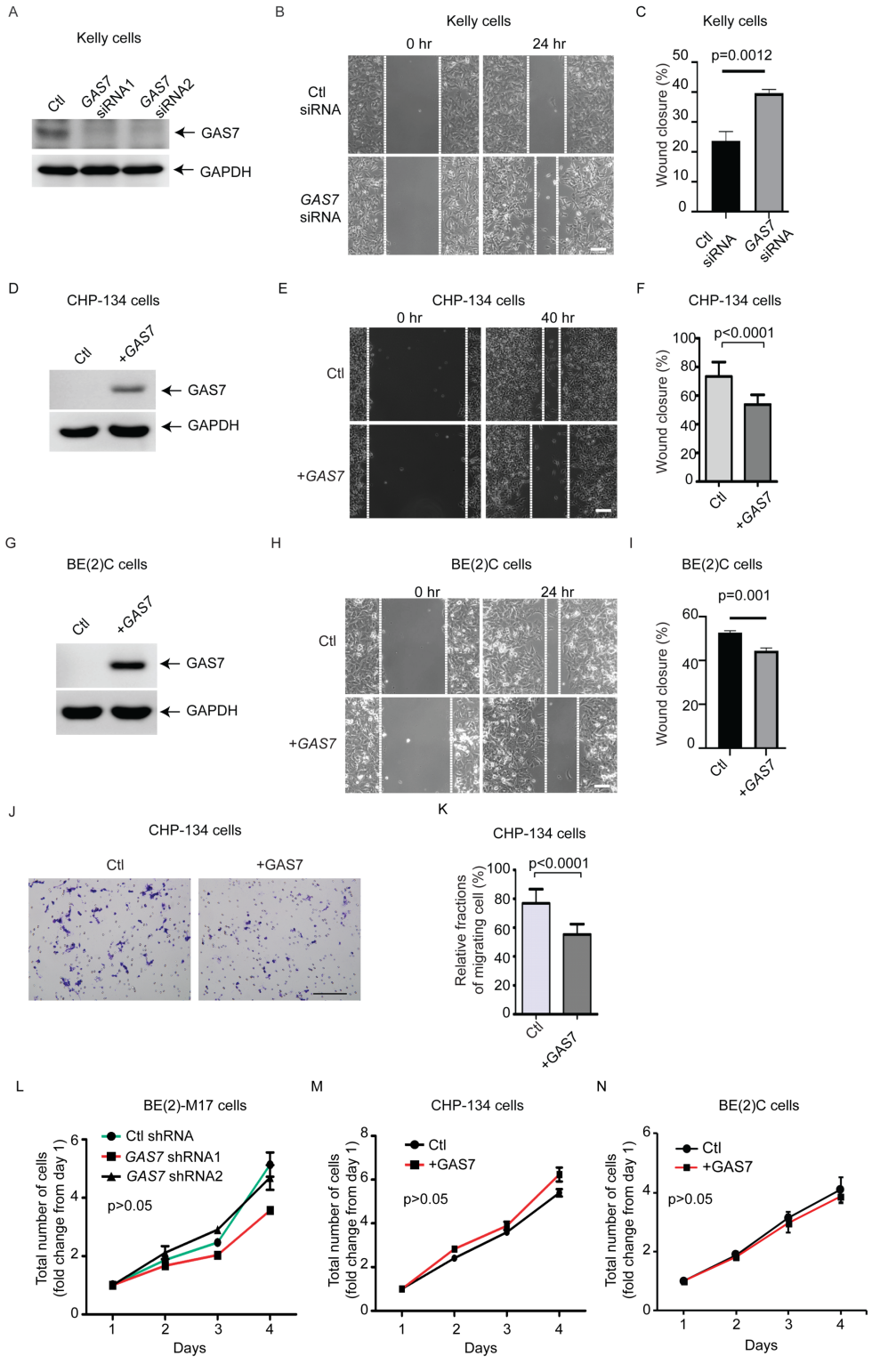

Supplementary Figure 4: Deregulation of *GAS7* expression affects the invasive and migratory properties of human NB cells with no significant impact on the growth of tumor cells during a short-period *in vitro* culture. (A) Immunoblotting of GAS7 expression in the Kelly NB cells after transfection with *GAS7* siRNAs. Levels of GAPDH expression served as a loading control. **(B,C)** Wound-healing assay of Kelly cells transfected with control siRNA (Ctl siRNA) or *GAS7* siRNA. (B) Representative bright-field pictures at 0- or 24-hr time point. (C) Quantification of wound healing in area to which the cells migrated. Scale bar, 200µm. Data are presented as means ± SD of triplicate experiments, p=0.0012 by two-tailed *t* test. **(D)** Immunoblotting of GAS7 expression in the CHP-134 NB cells after stable overexpression of control (Ctl) or *GAS7* (+*GAS7*) lentiviral construct. Levels of GAPDH expression served as a loading control. (E,F) Wound-healing assay of CHP-134 NB cells with stable overexpression of control vector (Ctl) or *GAS7* (+*GAS7*) lentiviral construct. **(E)** Representative bright-field pictures at 0- or 40-hr time point. Scale bar, 200µm. **(F)** Quantification of wound healing in area to which the cells migrated. Data are presented as means ± SD of triplicate experiments; p<0.0001 by two-tailed *t* test. **(G)** Immunoblotting of GAS7 expression in the BE(2)C NB cells after stable overexpression of control (Ctl) or *GAS7* (+*GAS7*) lentiviral construct. Levels of GAPDH expression served as a loading control. (H,I) Wound-healing assay of BE(2)C NB cells with stable overexpression of control vector (Ctl) or *GAS7* (+*GAS7*) lentiviral construct. **(H)** Representative bright-field pictures at 0- or 24-hr time point. Scale bar, 200µm. **(I)** Quantification of wound healing in area to which the cells migrated. Data are presented as means ± SD of triplicate experiments; p=0.001 by two-tailed *t* test. (J,K) Transwell invasion and migration assay of the CHP-134 NB cells with stable overexpression of control vector (Ctl) or *GAS7* (+*GAS7*) lentiviral construct. **(J)** Crystal violet-stained migrated cells. Scale bar, 200µm. **(K)** Relative numbers of cells migrated through the membrane. Data are presented as means ± SD of triplicate experiments; p<0.0001 by two-tailed *t* test. **(L)** Growth of BE(2)-M17 cells infected with *GAS7* shRNA1 or *GAS7* shRNA2 was not significantly different from the cells infected with control shRNA (Ctl shRNA). **(M-N)** Growth of the CHP-134 (M) or BE(2)C (N) with stable overexpression of *GAS7* (+*GAS7*) was not significantly different from the cells overexpressing the control (Ctl) vector. Cell viability was measured every day for 4 days in the control cells or cells with stable knockdown or overexpression of *GAS7*. The data in all panels are means ± SD of triplicate experiments, p values determined by two-tailed *t* test.

Supplementary Figure 5

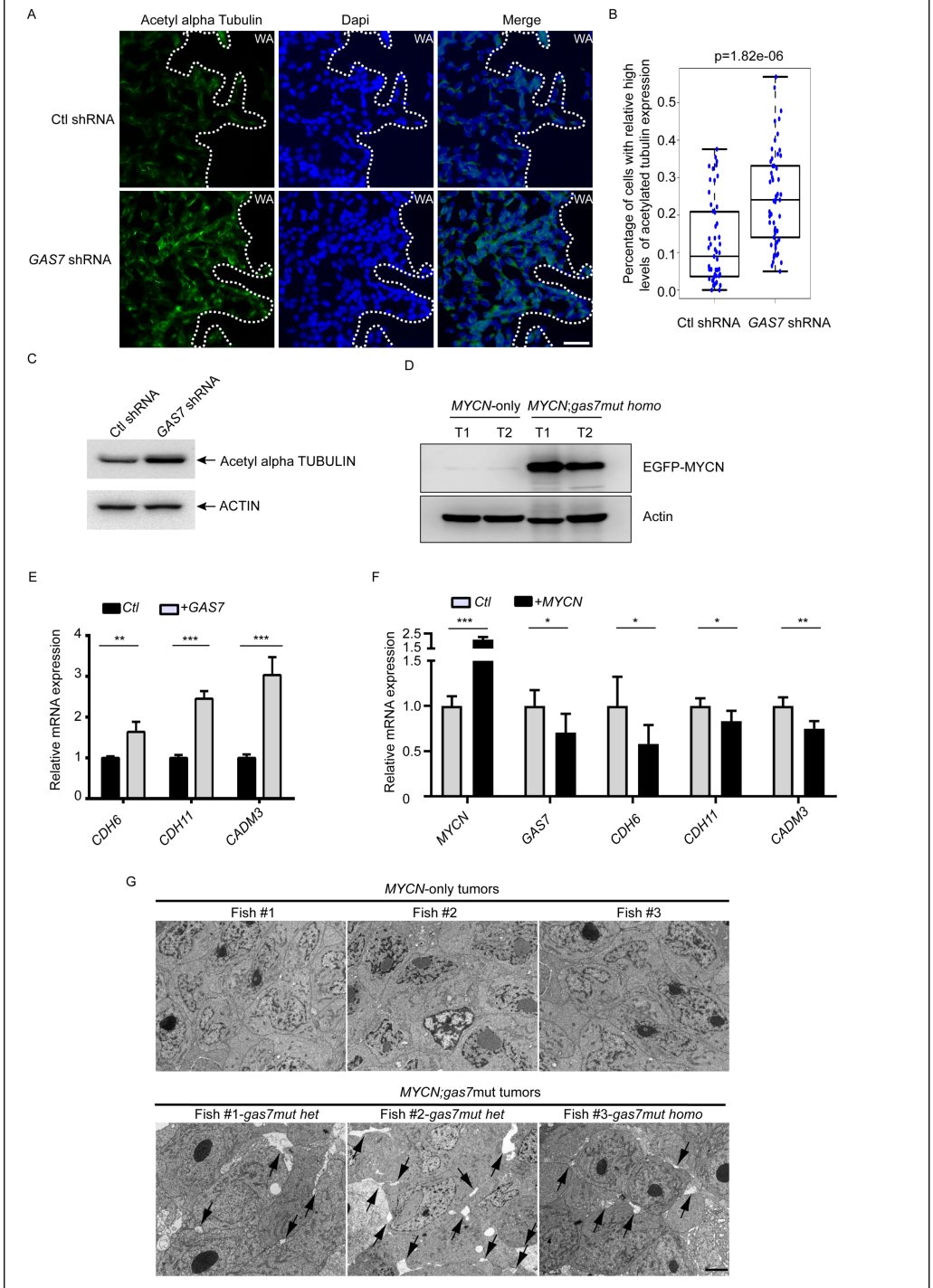

Supplementary Figure 5: Reduced *GAS7/gas7* expression affects microtubule dynamics and cell-cell adhesion in the context of *MYCN* overexpression. (A,B) Immunofluorescence staining of acetylated TUBULIN in BE(2)-M17 cells infected with control shRNA (Ctl shRNA, top panels) or *GAS7* shRNA (bottom panels). B. Quantification of percentage of cells with higher levels of acetylated TUBULIN expression in the control (Ctl shRNA) or *GAS7* shRNA knockdown cells (*GAS7* shRNA). WA, wound area; scale bar, 200μm. The data are presented as mean ± SD of duplicated experiments; p = 1.82e-06 by two-tailed t test. **(C)** Immunoblotting of acetylated TUBULIN in BE(2)-M17 NB cells infected with control shRNA (Ctl shRNA) or *GAS7* shRNA. The levels of ACTIN expression served as a loading control. **(D)** Immunoblotting of MYCN expression in two *MYCN*-only and two *MYCN;gas7mut homo* NBs. The levels of Actin expression served as a loading control. **(E-F)** Relative expression values of representative genes identified from enriched biological processes, including *CDH6*, *CDH11* and *CADM3*, or *GAS7* in CHP-134 or BE(2)-M17 cells transfected with control vector (Ctl), *GAS7* (+*GAS7*, E) or *MYCN* construct (+*MYCN*, F) by qRT-PCR analyses. All of the values were further normalized to the mean of expression of each given gene in the Ctl vector-overexpressing CHP-134 or BE(2)-M17 cells. The data are presented as means ± SD of triplicate experiments; *p < 0.05, **p < 0.01, ***p < 0.001 by two-tailed *t* test. **(G)** Electron microscopic analysis of three individual *MYCN*-only (top panel), *MYCN;gas7mut het* or *MYCN;gas7mut homo* (lower panel) NBs. Scale bar represents 2μm. Spaces among cells in *MYCN;gas7mut* tumor are highlighted by arrows (lower panel).

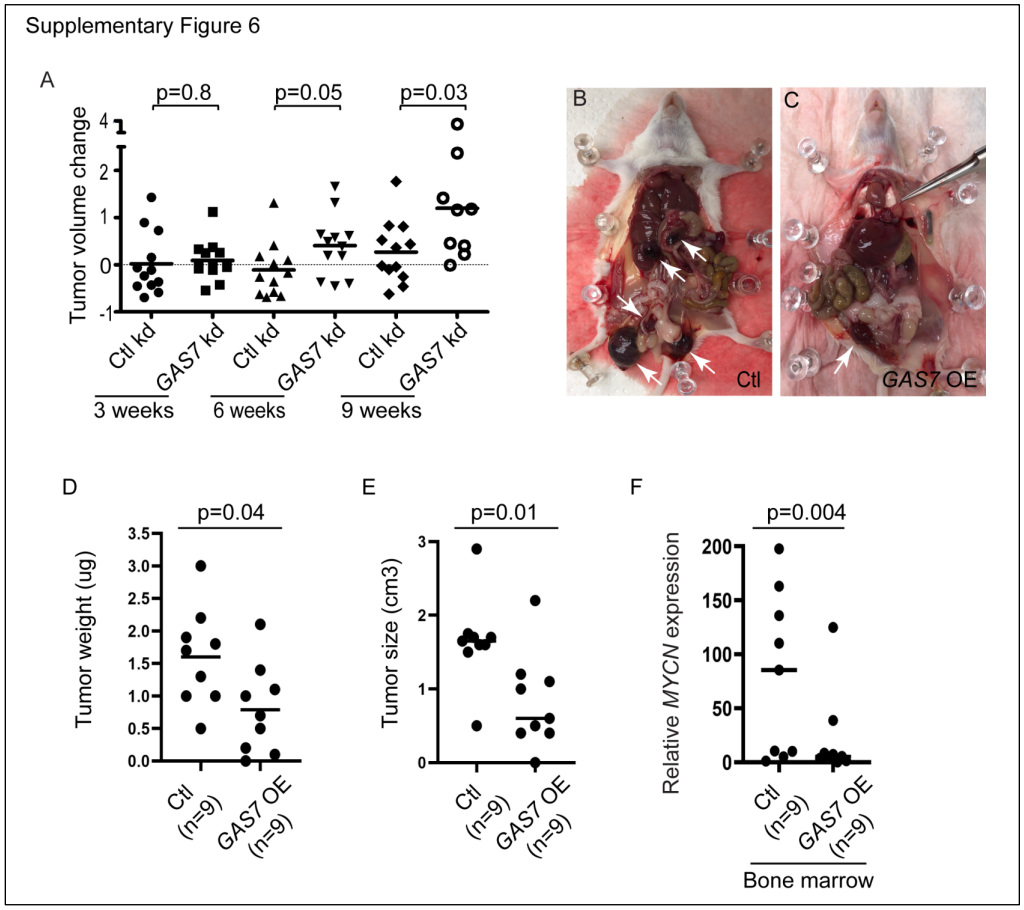

Supplementary Figure 6: Deregulation of *GAS7* expression alters the growth and metastatic ability of NB cells in xenografted mice. (A) Quantification of tumor volume changes in mice xenografted with control (Ctl kd) or *GAS7* knockdown (*GAS7* kd) BE(2)-M17 cells over 9 weeks of observation. Data are reported as mean values of combined primary and metastatic tumors from all live mice at given times (horizontal bars). P values were determined by log-rank test. **(B,C)** Representative images of mice injected with BE(2)C cells infected with control (Ctl, B) or *GAS7*-overexpressing construct (*GAS7* OE, C) at 4 weeks post-transplantation. **(D,E)** The weight (D) and size (E) of tumors dissected from mice injected with BE(2)C cells infected with control (Ctl) or *GAS7*-overexpressing construct (*GAS7* OE) at 4 weeks post-transplantation. **(F)** Relative expression of *MYCN* versus *Gapdh* in DNA extracted from bone marrow cells of mice transplanted with control or *GAS7*-overexpressing BE(2)C cells by Q-PCR analyses. The difference of abundance of *MYCN* in DNA isolated from bone marrow cells of mice transplanted with control vs. *GAS7*-overexpressing BE(2)C cells is significant at p=0.004 by two-tailed Wilcoxon signed-rank test.

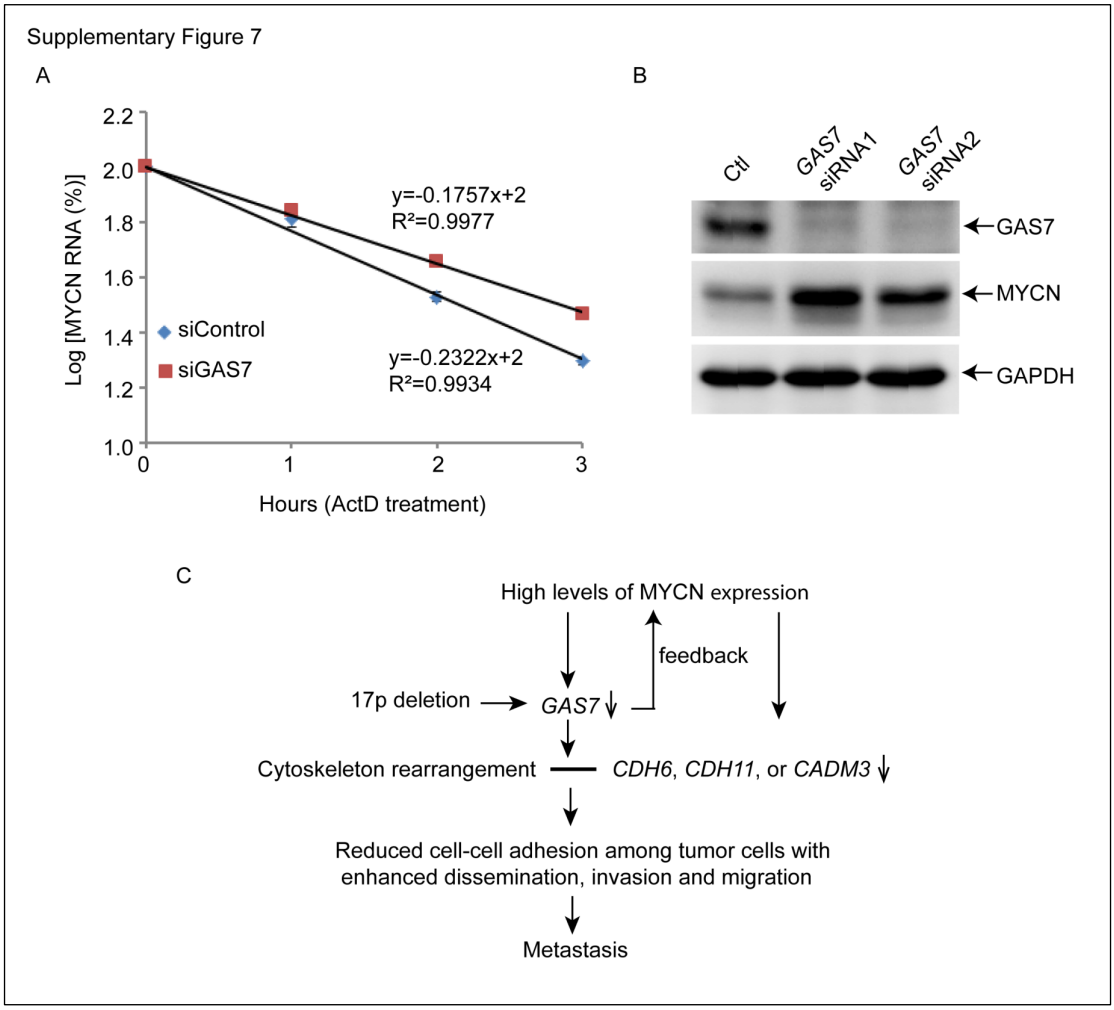

Supplementary Figure 7. Hypothetical model of MYCN-GAS7 feedback regulation in facilitation of tumor metastasis in high-risk NB. (A) Decay of *MYCN* mRNA in Kelly cells transfected with control (siControl) or *GAS7* siRNAs (siGAS7) after Actinomycin D (ActD) treatment. The relative expression levels of *MYCN* versus *SDHA* and *HPRT1* were determined by quantitative RT-PCR at each indicated time point from duplicated experiments. **(B)** Immunoblotting of MYCN and GAS7 expression in Kelly cells transfected with *GAS7* siRNAs. The levels of GAPDH expression served as a loading control. **(C)** Hypothetical model of MYCN-GAS7 role in the metastasis of high-risk NB. Amplification or overexpression of *MYCN* primes tumor cells for metastasis by downregulating the expression of *GAS7,* consequently the expression of cell adhesion molecules (such as *CDH6*, *CDH11* or *CADM3*) and the alteration of cytoskeleton, leading to metastasis. Moreover, reduced *GAS7* expression can increase MYCN expression which in turn enhances its transcriptional downregulation of key genes involved in cell-cell interaction to promote tumor dissemination and metastasis, as summarized above.

SUPPLEMENTARY METHODS

Genomic DNA Isolation and Genotyping

Embryos or tail fins were incubated in lysis buffer (1M Tris–HCl [pH 8.3], 1M KCl, 10% Tween 20, and 10% NP40) and subsequently treated with proteinase K (10 mg/ml) at 55°C overnight. After centrifuging at 12, 000 × g for 10 minutes at 4°C, the supernatant was subjected to PCR using primers described in Supplementary Table S2.

Fluorescence Activated Cell Sorting (FACS)

MYCN and *dβh:EGFP* embryos were dissected and digested with 0.5% trypsin (GIBCO, Grand Island, NY, USA) for 30 min at 37°C. A single-cell suspension was pelleted by centrifugation at 400 × g for 5 min, followed by washing twice with PBS and filtering with a 40-μm cell strainer. $EGFP^+$ cells were sorted with the BD FACSARIA III (BD Biosciences, San Jose, CA, USA) and subjected to RNA extraction.

RNA Extraction and Semiquantitative RT-PCR

Total RNA was extracted from zebrafish tumors or human NB cell lines using the Trizol reagent (Sigma-Aldrich). RNA was reverse-transcribed using the oligo (dT) primer and Superscript III reverse transcriptase (RT) (Invitrogen). The cDNA amplification was performed using SYBR Premix ExTaq kit (Takara, JP) with a Bio-Rad CFX Real-Time PCR Detection system (Hercules, CA). Sequences of primer sets are given in Table S2. All reactions were performed in triplicate. Quantitative data were calculated from the Ct-values for each reaction, with the mean reaction efficiency used for each primer pair. Data were normalized to the expression levels of *ACTIN* for human genes and the *elfa* for zebrafish genes, respectively.

Paraffin Sectioning and Immunostaining

Tumor-bearing fish were fixed with 4% paraformaldehyde and embedded in paraffin followed by sectioning and H&E staining at the Mayo Clinic Histology Core Facility in Arizona with standard protocols. Immunohistochemistry of paraffin sections was performed with a Leica BOND-MAX instrument and BOND™ reagents using primary antibodies against TH (Pel-Freez Biologicals Cat# P40101, RRID:AB_2313713, 1:500), GFP (Thermo Fisher Scientific, Cat# A-6455, RRID:AB_221570, 1:500) and Hu (Life Technologies, Cat# A-21271, RRID:AB_221448, 1:2000), according to the standard protocols. The stained sections were subsequently examined by pathologists in a blinded manner.

Electron Microscopy and Imaging

Fish tumors were fixed with 4% paraformaldehyde plus 1% glutaraldehyde fix in phosphate-buffered saline, pH 7.2. After fixation, tissues were stained with 1% osmium tetroxide and 2% uranyl acetate, then dehydrated through an ethanol series and embedded into Embed 812 resin. After 24-hr polymerization at 60°C, 0.1 μm ultrathin sections were post-stained with lead citrate. Micrographs were acquired with a JEOL1400 transmission electron microscope (Peabody, MA) operating at 80kV with a Gatan Orius camera and Digital Micrograph software (Pleasanton, CA).

Virus Production, Infection and Transfection

The *pLKO.1* lentiviral vectors containing *GAS7* shRNAs (TRCN0000013226 and TRCN0000013227) and control shRNA were purchased from Sigma. The *pLX304* lentiviral expression vector containing CDS of *GAS7* (Clone Id: ccsbBroad304_01948) was purchased from Dharmacon (1). The lentiviral constructs were cotransfected into 293T cells with packaging vectors, *psPAX2* (RRID:Addgene_12260) and *pMD2.G* (RRID:Addgene_12259), using FuGENE 6 reagent (Roche). Supernatants containing lentivirus were collected, filtered through a 0.45-mm filter, and infected with NB cells in the presence of polybrene (8 mg/mL). The infected cells were treated with puromycin or Blasticidin S for 4 days to remove any uninfected cells. To knockdown *GAS7* in Kelly cells, control siRNA (D-001810-10-05, Dharmacon or SIC001-10NMOL, Sigma) , *GAS7* siRNA (hs.Ri.GAS7.13.1, IDT) or *GAS7* siRNA (hs.Ri.GAS7.13.5, IDT) was transfected into cells on the first and second day after seeding, using lipofectamine RNAiMax at a final concentration of 10 nM.

Cell Invasion Assay

Cells were pelleted and resuspended in medium with 1% FBS before plating in Corning Matrigel invasion chambers in 24-well plates. Medium containing 10% FBS was filled outside the chambers. After incubation for indicated time, cells on the top surface of each insert were removed. The inserts were then washed twice with PBS followed by crystal violet staining for 20 min. After being rinsed with water three times, the membranes of the chambers were mounted on slides and observed with a light microscope. Experiments were independently repeated three times.

Wound-Healing Assay

Cells were seeded in wells of 6-well plates and incubated to 90-100% confluence. Sterile yellow pipette tips were used to create wounds. After being rinsed with PBS three times, cells were further cultured in RPMI1640 medium supplemented with 10% FBS. At least 20 wound fields were imaged with two-hour interval. Assays were repeated three times for each cell line. Cells migrating into the wound area were quantified by calculating the percentage of the original wound area covered by migrating cells.

Immunofluorescence Staining and Quantification of Stained Cells

Control or *GAS7* shRNA-infected BE(2)-M17 cells were seeded in 6-well plates and scratched with sterile yellow pipette tips to create wounds as mentioned above. When the wounds were about to close, cells were fixed with 100% methanol for 10 min at −20°C, followed by three times of wash with PBS, 60 min of blocking, overnight incubation with primary antibody against acetylated-TUBULIN (Sigma, Cat# T7451, RRID:AB_609894, 1:1000) at 4°C and 1 hour incubation with Alexa Fluor 488-conjugated 2nd antibody (Invitrogen, Cat# A-11029, RRID:AB_138404, 1:500) at room temperature. Assays were repeated two times and at least 20 wound fields were imaged for each cell line per assay. Cells migrating into the wound area with fluorescence intensity over a threshold of 85 (in a range of 0~255 in histogram) were quantified and the percentage of these cells among total numbers of cell in the field (quantified based on dapi staining) were calculated.

Immunoblotting

Protein lysates were prepared in prechilled RIPA buffer (150 mM NaCl, 50 mM Tris-HCl pH 8, 5 mM EDTA, 50 mM PMSF, 1% IGEPAL CA-630, 0.5% sodium deoxycholate, 0.1% SDS and 1x Halt protease inhibitor cocktail). Protein concentrations were determined by Bradford assay (BioRad). About 80 mg of protein lysates were separated by electrophoresis on 4-12% Bis-Tris Protein Gels (Thermo Fisher Scientific), then transferred to PVDF membranes (Millipore) and probed overnight at 4°C with the following primary antibodies: anti-GAS7 (Aviva Systems Biology, Cat# ARP47759_T100, RRID:AB_1042574, 1:100), anti-MYCN (Santa Cruz, Cat# sc-53993, RRID:AB_831602, 1:1000), anti-GAPDH (GeneTex, Cat# GTX100118, RRID:AB_1080976, 1:5000), anti-alpha TUBULIN (abcam, Cat# ab18251, RRID:AB_2210057, 1:1000). Primary antibody binding was visualized on X-ray film using anti-mouse (Cell Signaling, Cat# 7076, RRID:AB_330924, 1:5000) or anti-rabbit (Cell Signaling, Cat# 7074, RRID:AB_2099233, 1:5000) secondary antibodies together with Pierce ECL western blotting substrate or SuperSignal West chemiluminescent substrates (Thermo Fisher Scientific).

Dual Chromatin Immunoprecipitation Assay

Dual ChIP cross-linking was performed following previously description (2, 3). The antibodies used in this assay were MYCN (Santa Cruz, Cat# sc-53993, RRID:AB_831602), IgG (Upstate, Cat# 12-371, RRID:AB_145840) and SP1 (Upstate, Cat# 07-645, RRID:AB_310773). Specific pairs of primers used for semiquantitative PCR are listed in Supplementary Table S3.

Luciferase Assay

The promoter region of *GAS7* (−1097/+644) was amplified by PCR and cloned into the *pGL3-basic* vector (Promega, Cat# E1751). The Renilla–TK vector (Promega, Cat# E2241) served as an internal control. The activities of *firefly* and *Renilla* luciferase were measured with the Dual Luciferase Assay kit (Promega), according to the manufacturer's instructions.

RNA-Sequencing and Bioinformatics Analysis

The RNA-sequencing analysis of zebrafish tumors is described in full in our previous report (4). Briefly, Fastq files of pair-end RNA-sequencing reads were aligned with Tophat 2.0.14 (RRID:SCR_013035) to the UCSC reference genome danRer10 using Bowtie2 2.2.6 (RRID:SCR_005476) with default parameters (5, 6). Gene level counts were obtained with FeatureCounts 1.4.6 (RRID:SCR_012919) from the SubRead package (RRID:SCR_009803) with gene models from corresponding UCSC annotation packages (7). Gene symbols were mapped to their human homologues using the homology information from Mouse Genome Informatics (http://www.informatics.jax.org/homology.shtml, RRID:SCR_017517), and only genes mapped to human homologues were used for downstream analysis. Differential expression analysis on the mapped human homologues was performed with R package DESeq2 1.10.1 (RRID:SCR_015687) (8). In gene set enrichment analysis (GSEA), the whole transcriptome was ranked by fold changes according to Subramanian et al (9) against the gene sets from the MSigDB database (RRID:SCR_016863) (10).

To compare functional annotation with a human transcriptomic profiling dataset containing 498 samples (11), we downloaded the expression matrix and sample annotation of this dataset from the R2 database ['R2: Genomics Analysis and Visualization Platform (http://r2.amc.nl)'].

Only data annotated as *MYCN*-amplified high-risk NBs were included in our analysis. Pearson correlation was applied to identify genes whose expression levels are positively associated with that of *GAS7*. A Pearson correlation-ranked gene list was used to perform GSEA, with enriched pathways having a p-value <0.05 were considered significant.

TALEN-Mediated Mutagenesis

The TALENs were designed using the Mojo Hand Version 2 software [available online at http://www.talendesign.org (12)]. The *gas7* TALEN binding sites were positioned around a 15-bp spacer sequence containing a FokI restriction enzyme site. The TALEN vectors were generated by the Golden Gate method with a pT3TS-GoldyTALEN destination vector (13, 14). The TALEN mRNAs were synthesized as previously described (13). A volume of 1 nL (30 ng/μL) of TALEN mRNA was injected into embryos at the one-cell stage to develop knockout fish line.

Tumor Xenograft Assay

For transplantation assays, the same number of BE(2)M17 and BE(2)C NB cell lines infected with a luciferase construct and *GAS7* shRNA, control shRNA, a *CMV promoter-mediated-GAS7* expression vector or a control vector were injected intraperitoneally into SCID mice through a 0.5-inch 16-gauge needle. Briefly, about 200μl of cell suspension (~1×10^6 cells per animal) in 1:1 ratio of Matrigel (BD Biosciences, San Jose, CA, USA) and PBS were injected into the abdominal cavities of the SCID mice. The Injected mice were monitored regularly by Xenogen imaging system and scarified for further analyses at 11 weeks or 4 weeks post-transplantation, respectively.

References:

1. Yang X, Boehm JS, Yang X, Salehi-Ashtiani K, Hao T, Shen Y, et al. A public genome-scale lentiviral expression library of human ORFs. Nature methods. 2011;8(8):659-61.
2. Iraci N, Diolaiti D, Papa A, Porro A, Valli E, Gherardi S, et al. A SP1/MIZ1/MYCN repression complex recruits HDAC1 at the TRKA and p75NTR promoters and affects neuroblastoma malignancy by inhibiting the cell response to NGF. Cancer research. 2011;71(2):404-12.
3. Zeng PY, Vakoc CR, Chen ZC, Blobel GA, Berger SL. In vivo dual cross-linking for identification of indirect DNA-associated proteins by chromatin immunoprecipitation. BioTechniques. 2006;41(6):694, 6, 8.
4. Zhu S, Zhang X, Weichert-Leahey N, Dong Z, Zhang C, Lopez G, et al. LMO1 Synergizes with MYCN to Promote Neuroblastoma Initiation and Metastasis. Cancer cell. 2017;32(3):310-23 e5.
5. Kim D, Pertea G, Trapnell C, Pimentel H, Kelley R, Salzberg SL. TopHat2: accurate alignment of transcriptomes in the presence of insertions, deletions and gene fusions. Genome biology. 2013;14(4):R36.
6. Langmead B, Salzberg SL. Fast gapped-read alignment with Bowtie 2. Nat Meth. 2012;9(4):357-9.
7. Liao Y, Smyth GK, Shi W. The Subread aligner: fast, accurate and scalable read mapping by seed-and-vote. Nucleic Acids Research. 2013;41(10):e108-e.

8. Love MI, Huber W, Anders S. Moderated estimation of fold change and dispersion for RNA-seq data with DESeq2. Genome Biology. 2014;15(12):550.
9. Subramanian A, Tamayo P, Mootha VK, Mukherjee S, Ebert BL, Gillette MA, et al. Gene set enrichment analysis: a knowledge-based approach for interpreting genome-wide expression profiles. Proceedings of the National Academy of Sciences of the United States of America. 2005;102(43):15545-50.
10. Liberzon A, Subramanian A, Pinchback R, Thorvaldsdottir H, Tamayo P, Mesirov JP. Molecular signatures database (MSigDB) 3.0. Bioinformatics. 2011;27(12):1739-40.
11. Consortium SM-I. A comprehensive assessment of RNA-seq accuracy, reproducibility and information content by the Sequencing Quality Control Consortium. Nature biotechnology. 2014;32(9):903-14.
12. Neff KL, Argue DP, Ma AC, Lee HB, Clark KJ, Ekker SC. Mojo Hand, a TALEN design tool for genome editing applications. BMC bioinformatics. 2013;14:1.
13. Bedell VM, Wang Y, Campbell JM, Poshusta TL, Starker CG, Krug RG, 2nd, et al. In vivo genome editing using a high-efficiency TALEN system. Nature. 2012;491(7422):114-8.
14. Cermak T, Doyle EL, Christian M, Wang L, Zhang Y, Schmidt C, et al. Efficient design and assembly of custom TALEN and other TAL effector-based constructs for DNA targeting. Nucleic acids research. 2011;39(12):e82.